Essential Cytoplasmic Role of the Histone Lysine Methyltransferase Setdb1 in Post-Transcriptional Regulation in Embryonic Stem Cells

Roberta Rapone, Laurence Del Maestro, Costas Bouyioukos, Sonia Albini, Paola Cruz-Tapias, Véronique Joliot, Bertrand Cosson, Slimane Ait-Si-Ali

Essential Cytoplasmic Role of the Histone Lysine Methyltransferase Setdb1 in Post-Transcriptional Regulation in Embryonic Stem Cells

Roberta Rapone
Université de Paris - CNRS
Laurence Del Maestro
Université de Paris - CNRS
Costas Bouyioukos
Université de Paris - CNRS
Sonia Albini
Université de Paris - CNRS
Paola Cruz-Tapias
Université de Paris - CNRS
Véronique Joliot
Université de Paris - CNRS
Bertrand Cosson
Université de Paris, Epigenetics and Cell Fate, UMR7216, CNRS https://orcid.org/0000-0003-3401-7137
Slimane Ait-Si-Ali (slimane.aitsiali@u-paris.fr)
Université de Paris - CNRS

Article

Keywords: Setdb1, cytoplasm, ES cells, Trim71, post-transcriptional regulation

Posted Date: February 5th, 2021

DOI: https://doi.org/10.21203/rs.3.rs-145869/v1

Essential Cytoplasmic Role of the Histone Lysine Methyltransferase Setdb1 in Post-Transcriptional Regulation in Embryonic Stem Cells

AUTHORS

Roberta RAPONE, Laurence DEL MAESTRO, Costas BOUYIOUKOS, Sonia ALBINI, Paola CRUZ-TAPIAS, Véronique JOLIOT, Bertrand COSSON*, Slimane AIT-SI-ALI*

AFFILIATION

Université de Paris, Epigenetics and Cell Fate, CNRS UMR7216, F-75013 Paris, France

***CORRESPONDING AUTHORS:** slimane.aitsiali@u-paris.fr; Tel.: +33-(0)1-5727-8919 and bertrand.cosson@u-paris.fr

Abstract

Embryonic stem cells (ESCs) fate is regulated both at transcriptional and post-transcriptional levels. Indeed, several studies showed that, in addition to gene transcription, mRNA stability and protein synthesis are finely tuned and strongly control the ESCs pluripotency and fate changes. An increasing number of RNA-binding proteins (RBPs) involved in post-transcriptional and translational regulation of gene expression has been identified as regulators of ESC identity. The major lysine methyltransferase Setdb1 is essential for the self-renewal and viability of ESCs. Setdb1 was primarily known to methylate the lysine 9 of histone 3 (H3K9) in the nucleus, where it regulates chromatin functions. However, Setdb1 is also massively localized in the cytoplasm, including in mouse ESCs, where its role remains unknown. Here we show that the cytoplasmic Setdb1 (cSetdb1) is essential for the survival of mESCs. Functional assays further demonstrate that cSetdb1 regulates gene expression post-transcriptionally, affecting the abundance of mRNAs and the rate of newly synthetized proteins. A yeast-two-hybrid assay shows that cSetdb1 interacts with several regulators of mRNA stability and protein translation machinery, such as the ESCs-specific E3 ubiquitin ligase and mRNA silencer Trim71/Lin41. Finally, proteomic analyses reveal that cSetdb1 is required for the integrity of Trim71 complexes involved in mRNA metabolism and translation. Altogether, our data uncover the essential cytoplasmic function of a firstly supposed nuclear “histone” lysine methyltransferase, Setdb1, and provide new insights into the cytoplasmic/post-transcriptional regulation of gene expression mediated by a key epigenetic regulator.

Key words: Setdb1, cytoplasm, ES cells, Trim71, post-transcriptional regulation

Embryonic stem cells (ESCs) fate is influenced by transcriptional and post-transcriptional regulation of gene expression. The role of transcription factor regulatory networks in combination with chromatin modifying proteins in ESCs fate have been extensively studied. Increasing evidences show that also mRNA stability and mRNA translation are finely tuned and strongly control the pluripotency and the fate of ESCs (Gabut et al., 2020). Moreover, an increasing number of RNA-binding proteins (RBPs) involved in post-transcriptional and translational regulation of gene expression has been identified and described as regulatory of ESC identity (Kwon et al., 2013; Ye and Blelloch, 2014; You et al., 2015).

Setdb1 (also called ESET/KMT1E) is a histone 3 lysine 9 (H3K9) lysine methyltransferase (KMT) which belongs to the SUV39 family, and a major epigenetic regulator of transcriptional gene repression. *Setdb1* knockout (KO) is lethal in mice at the peri-implantation stage (Dodge et al., 2004). Setdb1 is essential for the survival of mESCs and it influences ESCs identity, pluripotency and self-renewal (Bilodeau et al., 2009; Lohmann et al., 2010; Yeap et al., 2009). Setdb1 is also required for the cell survival, pluripotency maintenance and terminal differentiation of many progenitor cell types. Setdb1 is necessary for the survival of spermatogonial progenitors in mice (An et al., 2014) and a mesenchyme-specific *Setdb1* knock-out resulted in an increase of articular chondrocytes terminal differentiation (Lawson et al., 2013). Furthermore, Setdb1 is crucial for early neurogenesis in mice by promoting proliferation and cell survival (Tan et al., 2012). In contrast, Setdb1 is crucial for osteoblast differentiation during bone development (Lawson et al., 2013) and is involved in the terminal differentiation of skeletal muscle adult stem cells (Beyer et al., 2016) and growth plate chondrocytes (Yang et al., 2013).

Setdb1 shows unusual distinct subcellular and subnuclear distributions, including in ESCs (Beyer et al., 2016; Loyola et al., 2006; Schultz et al., 2002; Yeap et al., 2009), but the meaning of the different Setdb1 subcellular localisations remains mostly unknown. Although, the role of nuclear Setdb1 in transcription regulation, especially in mESCs, has been extensively studied, its cytoplasmic role remains elusive.

Since Setdb1 is essential for ESCs, we first asked whether cytoplasmic Setdb1 (cSetdb1) is required for the survival of ESCs. Our cellular studies showed that the loss of normal cytoplasmic localization of Setdb1 in ESCs lowers the cell amount and increases the number of apoptotic cells. The loss of cSetdb1 affects specific mRNA abundance and the overall rate of newly synthetized proteins. Biochemical protein-protein interaction studies unraveled that cSetdb1 interacts with several regulators of mRNA processing and translation, among which the ESC-specific RNA binding protein (RBP) Trim71/Lin41. Proteomic studies further demonstrated that cSetdb1 is required for the integrity of Trim71 protein complexes. Taken together, our results suggest a new fundamental role of

cSetdb1 in mESCs, which influences post-transcriptional regulation of gene expression and provide new insights into the cytoplasmic regulation of gene expression mediated by a key epigenetic regulator.

Results

Cytoplasmic Setdb1 is an active lysine methyltransferase required for the survival of embryonic stem cells

Setdb1 is essential for mouse embryonic stem cells survival (mESCs, see introduction). While Setdb1 function, extensively studied in mESCs, has been always associated with its nuclear role, it has been shown that Setdb1 localizes also in the cytoplasm. However, the importance and the function of cytoplasmic Setdb1 (cSetdb1) in mESCs has never been investigated.

To address the cytoplasmic role of Setdb1 in mESCs, we used the TT2 mESCs which have been genetically modified to induce an acute *Setdb1* knockout (KO) by tamoxifen (TA). Indeed, an acute Setdb1 protein depletion was obtained from 48h post-TA treatment (**Fig 1A**). We also used inducible TT2 *Setdb1* KO cells where exogenous wild-type Setdb1 (KO+WT) or enzymatically-dead point mutant (KO+CA) were stably expressed in the nucleus and in the cytoplasm (**Fig 1B**). Using these cell systems, we first investigated whether cSetdb1 is enzymatically active. To this end, we performed an immunoprecipitation (IP) of Setdb1 from the cytoplasmic fractions of Ctr, KO, KO+WT or KO+CA mESC lines, using anti-Setdb1 antibody (Ab, **Fig 1C**). We used the IP products in an *in vitro* radioactive methylation assay using core histones as a substrate and radioactive S-Adenosyl Methionine (SAM) as methyl donor. We observed an enzymatic activity towards H3 in the Ctr and KO+WT conditions, and, as expected, not in KO and KO+CA (**Fig 1C**). Since the immunoprecipitates from KO and CA Setdb1 do not show any detectable methyltransferase activity (**Fig 1C**), we deduced that previous detected signals were specific for Setdb1. Thus, mESCs cSetdb1 is enzymatically active.

To investigate the role of cSetdb1 in mESCs, we generated an inducible *Setdb1* KO cells where Setdb1 expression is stably rescued only in the nucleus (KO+NLS) by adding an artificial strong nuclear localization signal (NLS) to the N-terminal part of the protein (**Fig 1B and 1D).** *Setdb1* depletion is known to cause growth defects in ESCs (Fisher et al., 2017), but the importance of Setdb1 cytoplasmic function has never been specifically examined. To this end, we first performed an apoptosis test using Annexin V-FITC/IP staining in KO and KO+NLS cells, compared to Ctr and KO+WT cells, after a long-term acute *Setdb1* KO (96h of TA treatment). As expected, we found almost twice more apoptotic cells in early stage (Annexin V+) and late stage (Annexin V and Propidium Iodide-PI+) of apoptosis upon acute *Setdb1* depletion (KO) compared to control (Ctr) (**Fig 1E**). Rescue of WT Setdb1 (KO+WT) restored the normal apoptotic index, while the expression of Setdb1 only in the

nucleus (KO+NLS), did not (**Fig 1E**), showing an increase in the number of apoptotic cells. To go further, we quantified the number of attached cells, which are living (trypan blue-positive). In accordance with the previous result, we observed a significant decrease in the number of KO and KO+NLS attached cells, compared to control KO+WT cells (**Fig 1F**). In addition, KO+NLS cells show less viability than KO+WT cells (**Fig 1F and S1A**). To further check if cSetdb1 is essential in ESCs, we looked after 6-days of TA treatment. Our data showed that the expression of nuclear-only Setdb1 exacerbated even more the number of apoptotic cells and lowers the number of attached cells (KO+NLS, **Fig 1G**). Moreover, by immunofluorescence, an increase in cleaved caspase-3 was detected in KO cells (**Fig S1B**).

Together, these data highlight the importance of cytoplasmic Setdb1 for ESCs survival.

Cytoplasmic Setdb1 regulates the abundance of mRNAs and newly synthetized proteins

Setdb1 in the nucleus regulates chromatin functions affecting transcription regulation in ESCs (Bilodeau et al., 2009; Yeap et al., 2009). We wondered whether cSetdb1 could influence gene expression at post-transcriptional level considering its importance in the regulation of protein abundance and ESC identity (Gabut et al., 2020; Schwanhausser et al., 2011). First, we looked at the amount of mRNAs, *via* RNAseq assay after ribodepletion, in KO+NLS compared to KO+WT mESCs cells. First, the PCA analysis showed that the three KO+NLS replicates were well defined and appear to form a distinct group from the KO+WT replicates (**Fig S2A**). 291 mRNAs were found differentially abundant in KO+NLS compared to KO+WT cells (**Fig 2A** and **Table 1**); of those genes, 76 were less abundant and 215 more abundant. While the role of Setdb1 in regulating gene expression has been always associated with its nuclear roles, our RNA-seq data suggest that cSetdb1 is also involved in gene expression regulation, at the mRNA transcript abundance level.

Gene ontology (GO) analysis for biological processes showed that most of differentially abundant mRNAs are enriched in gene categories related to Setdb1 phenotypes in mice (http://www.informatics.jax.org/marker/MGI:1934229). Notably, embryogenesis, including development (vascular, reproductive, placenta and somite development), tissue morphogenesis (including also branchial, epithelial and placenta morphogenesis), segmentation and regulation of cellular response to growth factor stimuli (**Fig. 2B**). In particular, we identified more abundant mRNAs related to reproductive and placenta development (such as *Gcm1* and *Tex19.1)* and to vascular, vessel development and angiogenesis *(such as Gpx1, Egr3, Adm and Enpp2*). Moreover, in line with the phenotype that we observed in absence of cSetdb1, we found, less abundant mRNAs associated with cell proliferation and cell survival, including *Dab2*, *kit*, *Fgf1* and *Pdgfra* (**Fig. 2B**). Further, enrichment analysis for biological processes and biological pathways, showed that the differentially abundant mRNAs are enriched in gene categories related to extracellular matrix (EM),

including EM organization, collagen formation and multimerization and cell adhesion (**Fig. 2C**). In particular we identified less abundant mRNAs related to EM structure/organization (such as collagen genes *Col23a1*, *Col4a1* and *Col4a2*) and more abundant mRNAs related to EM degradation (such as the matrix metalloproteinases *Mmp12*, *Mmp9* and *Mmp25*). All these categories and pathways are notably involved in ESCs self-renewal, proliferation and differentiation, thus associated with ESCs identity.

Interestingly, in accordance with the enrichment analysis, KO+NLS ESCs showed more spread distribution and less compact clones compared to KO+WT control ESCs, a phenotype characteristic of more committed cells (**Fig S2B**).

All these data show that in mESCs cSetdb1 affects the abundance of mRNAs mainly involved in development and cell adhesion, and suggest a loss of ESC state and a potential acquisition of a differentiated phenotype upon the depletion of Setdb1 cytoplasmic function.

Although Setdb1 was shown to be associated with ribosomes (Rivera et al., 2015), the possible role of Setdb1 in translation regulation has not been investigated. Thus, to pursue the study of the role of cSetdb1 in post-transcriptional gene expression control, we checked its potential participation in protein translation regulation. To this end, we performed a SUnSET assay, a non-radioactive method to quantify the amount of newly synthetized proteins (Schmidt et al., 2009), which mirrors ongoing protein synthesis through puromycin incorporation. We acutely depleted *Setdb1* in ESCs after 48h of tamoxifen treatment, a timepoint which does not alter the viability (**Fig S2C**), neither proliferation (**Fig S2D**), size and granularity of the cells (**Fig S2E**), rRNAs level (**Fig S2F**) or RNA synthesis (**Fig S2G**). The SUnSET assay specifically showed that an early acute *Setdb1* depletion (KO) affects ongoing protein synthesis, revealing a statistically significant almost 40% decrease in the amount of newly synthetized proteins, compared to control cells (Ctr) (**Fig 2D**). This phenotype is rescued by WT Setdb1 in KO+WT ESCs. However, very interestingly, the expression of nuclear-specific Setdb1 in KO+NLS ESCs did not rescue the protein synthesis defect, showing a statistically significant 42% decrease in the amount of newly synthetized proteins in KO+NLS compared to KO+WT ESCs **(Fig. 2D)**.

Together, the SUnSET assay and the rescue experiments suggest that the loss of Setdb1 in the cytoplasm affects the amount of newly synthetized proteins, therefore that cSetdb1 is required for protein synthesis in ESCs. Altogether, our results of RNA-seq, enrichment analysis and protein synthesis show that cSetdb1 plays key roles in post-transcriptional regulation of gene expression in ESCs, influencing mRNA abundance and the synthesis of proteins.

Cytoplasmic Setdb1 interacts with Trim71, a mESC-specific regulator of gene expression

We next sought to decipher the molecular mechanism(s) through which cSetdb1 post-transcriptionally affects gene expression. To this end, we conducted a yeast two-hybrid assay (Y2H,

performed by Hybrigenics Services, France) to identify potential cSetdb1 protein partners. We used as bait the full-length WT mouse Setdb1 cDNA, screened against a mESC cDNA library. Interestingly, the Y2H assay showed that Sedb1 interacts with several regulators of mRNA stability and translation (not shown). Among other proteins, our data assigned a robust and high-fidelity score to the interaction between Setdb1 and the RNA-binding protein and mRNA silencer Trim71 (also called Lin41), specifically expressed in ESCs. We confirmed this interaction by 1-by-1 Y2H assay (**Fig. 3A**). The mESC-specific RNA-binding protein Trim71 has a double function: it is a E3 ubiquitin ligase and it regulates gene expression post-transcriptionally. Notably, Trim71 localizes to Processing bodies (P-bodies), where mRNA repression occurs, and it is involved in the regulation of mRNA stability and translation (Chang et al., 2012; Loedige et al., 2013; Torres-Fernandez et al., 2019). The Y2H assay showed that the Setdb1/Trim71 interaction is overlapping the coiled-coil domain of Trim71 (**Fig. 3A**), which is required for Trim71 to repress mRNA function (Loedige et al., 2013). The interaction between cSetdb1 and Trim71 was confirmed by co-immunoprecipitation in mESCs of ectopically expressed proteins (**Fig. 3B**, left), and of exogenous Trim71 and endogenous Setdb1 (**Fig. 3B**, right). Moreover, *in situ* interaction assay (PLA assay) verified that cSetdb1 interacts with Trim71 *in situ* in mESCs, strengthening our data (**Fig. 3C, Video S1**). Since Trim71 is a E3 ubiquitin ligase, we wondered whether the interaction between Setdb1 and Trim71 affects their reciprocal protein stability. Acute *Setdb1* depletion (KO) did not affect Trim71 protein level, and its known partner Ago2 (**Fig. S3C**), neither the siRNA-mediated depletion of endogenous Trim71 (Trim71 KD), modified Setdb1 protein level (**Fig. S3B**).

The coiled-coil domain of Trim71 is required for its colocalization with DCP1a and directs Trim71 to P-bodies, where mRNA repression occurs (Torres-Fernandez et al., 2019). We found that this domain mediates also the interaction with Setdb1 (**Fig. 3**). Furthermore, using PLA, we show a spatial close proximity between Trim71 and DCP1a, a mRNA decapping enzyme involved in mRNA stability known to co-localize, indicating a direct interaction through physical contact or close functional coupling between Trim71 and DCP1a (**Fig. 3D** and **S3A, Video S2**). These results suggest a functional link between Setdb1, Trim71 and DCP1a to regulate mRNA behavior in ES cells.

We then evaluated the functional significance of the cSetdb-Trim71 interaction by checking if Trim71-regulated mRNAs are also regulated by cSetdb1. Comparing our RNA-seq results (described in **Fig. 2A**) with the transcripts differentially regulated after knock-out of *Trim71* in mESCs (Welte et al., 2019), we found 93 mRNAs commonly regulated by cSetdb1 (Setdb1 NLS) and Trim71 (*Trim71* KO) (**Fig. 3E**), 18 of them linked to multicellular organismal reproductive process (top biological process category from our ontology analysis (in bold in: **Table1**).

Next, we wondered whether cSetdb1 could influence the abundance of selected Trim71 mRNA targets, mainly involved in cell proliferation and embryogenesis, including *Inhbb* and *Ccnd2* and

potential Trim71 targets, including *H60b* and *Ccnd1*. By RNA-seq and RT-qPCR we found that *Inhbb* and *H60b* are dysregulated in absence of *Setdb1* (KO) or upon the expression of the nuclear-specific Setdb1 (KO+NLS), compared to the controls (Ctr and KO+WT) (**Table 1** and **Fig. 3F**). By RT-qPCR we observed the same for *Ccnd1* and *Ccnd2* (**Fig. 3F**). Our data show that cSetdb1 and Trim71 co-regulate the abundance of common mRNAs.

Finally, as for Setdb1 (**Fig. 2D**), we wondered whether Trim71 could regulate the amount of newly synthetized proteins. Interestingly, the amount of newly synthetized proteins decreases in absence of Trim71 (Trim71 KD), compared to control (Ctr) (**Fig. 3G**) Our results show the involvement of Trim71 in ongoing protein synthesis in ESCs as for cSetdb1.

All together, these new data confirm the previously demonstrated role of Trim71 in the regulation of mRNAs stability and translation, and highlights a functional role of cSetdb1, associated to Trim71, in post-transcriptional regulation of gene expression.

Integrity of Trim71 complex(es), involved in mRNA stability and translation, is affected in the absence of Setdb1

Our data showed that Setdb1 is a cytoplasmic partner of the ESC-specific RNA-binding protein and mRNA silencer Trim71/Lin41. To better understand the functional relation between Setdb1 and Trim71, we wondered whether Setdb1 is essential for the integrity of Trim71 complex, therefore for its functions. To address this question, we performed a proteomic analysis on Trim71 complex(es) in absence of Setdb1. We immunoprecipitated the cytoplasmic GFP-tagged Trim71 (Trim71) and its specific partners in ESCs, where we acutely depleted *Setdb1* after 48h of tamoxifen treatment (KO), a timepoint which does not alter the viability, neither proliferation, size and granularity of the cells, rRNAs level or RNA synthesis (shown in **Fig. S2C-G**), and in control ESCs (ES) and we compared them to their corresponding GFP controls (Ctr) (**Fig. 4A-B**). Then, the purified Trim71 complexes were analyzed by mass spectrometry. After discarding the sample with low sum of intensity **(Fig. S4A)**, we filtered for proteins that were well represented in the immunoprecipitates; we then applied a scale to interval normalization to better compare the samples (see Material and Methods). As expected, the PCA analysis (**Fig. 4C**) separates well all Trim71 samples from all Ctr samples. We then performed an ANOVA multi-sample test, which conducted to the selection of 108 proteins that were found differentially present in at least 2 of the 4 conditions (**Fig. 4D**). In order to select the partners of Trim71 that could differentially bind to Trim71 after an acute *Setdb1* knockout (KO-Trim71 against ES-Trim71), we performed a Post-Hoc Tukey's HSD test. We found, as displayed on the heatmap (**Fig. 4E**), that some Trim71 partners are more or less associated with Trim71 in absence of Setdb1 (KO-Trim71) compared to control cells (ES-Trim71). Notably, the RNA-binding protein hnRNP-C and Hmgcs1 are more enriched in KO-Trim71 compared to ES-Trim71, and, conversely, Eif5a2, Elp3, Gnl3,

Ranbp10 and Smyd5 are less enriched in KO-Trim71 compared to ES-Trim71. Very interestingly, these proteins are mainly involved and associated with mRNA stability, ribosome biogenesis and translation regulation. These data illustrate that the profile of Trim71 partners, whereby Trim71 executes its cellular functions, is dependent on Setdb1 and provide important mechanistic hypothesis to explain the role of cSetdb1 on post-transcriptional regulation.

Altogether, these observations shed new light on Trim71 complex function in mRNA stability and translation, revealing the importance of Setdb1 for its architecture and confirming the intimate relation between Setdb1 and Trim71.

An RBP partner of Trim-71, hnRNP-C, regulates the abundance level of key mRNAs involved in the control of cell fate

We have shown for the first time that the RNA-binding protein hnRNP-C, known to be involved in mRNA turnover and translation, is a member of Trim71 complex. Furthermore, we found the RBP hnRNP-C associates more with Trim71 in absence of cSetdb1 (**Fig. 4E**), highlighting a Setdb1-dependent interaction between hnRNP-C and Trim71. Therefore, we wondered whether there is a functional correlation between cSetdb1 and hnRNP-C; we checked if some of the mRNAs regulated by cSetdb1 are targets of hnRNP-C. 21 of the mRNAs found associated to hnRNP-C by eCLIP assay (Van Nostrand et al., 2016) are among the mRNAs differentially abundant in absence of cSetdb1 (**Fig. 4F**). Interestingly, 6 of them are implicated in Wnt signaling pathway, notably *GPC6*, *KANK1*, *CCNY*, *PRKAA2*, *HMGA2* and *Myc*. The last three are also implicated in cell cycle arrest. C-Myc is a known transcription factor, required for ESC self-renewal, maintenance of mESC identity and iPSC reprogramming. In addition to eCLIP assay, the scanning of all mouse 5' and 3'UTRs for hnRNP-C hits, through an established online prediction tool RBPmap, has identified that the mouse Myc, as the human, is a hnRNP-C target through its 5'UTRs (**Fig. S4B**). It has been shown that hnRNP-C binds human c-Myc mRNA on 5'UTR, regulating c-Myc translation level (Kim et al., 2003). Our data suggest that cSetdb1 would influence the c-Myc levels through hnRNP-C. In conclusion, we found interesting mRNAs regulated by cSetdb1 that are also hnRNP-C targets, strengthening our hypothesis concerning the functional correlation between hnRNP-C and cSetdb1 on post-translation regulation of gene expression.

Finally, we have performed a predictive analysis to check for the binding profile of hnRNP-C on the mRNAs regulated by cSetdb1 (mRNAs described in **Fig. 2** and **Table 1**). Indeed, having a well characterized hnRNP-C RNA binding motif, we performed a stringent computational prediction using RBPmap (see Materials and Methods), to scan the 5' and 3'UTRs of the 291 differentially abundant mRNAs found in absence of cytoplasmic Setdb1 by our RNA-seq for hnRNP-C binding motifs targets. Out of the 157 3'UTRs that we managed to retrieve from ENSEMBL (Materials and Methods), most

(128) were identified as potential targets of hnRNP-C (**Fig 4G** and **Table 2**). In the quest to more finely dissect the function and role of hnRNP-C in the absence of cytoplasmic Setdb1 in mESCs, we clustered the gene expression correlations of all the 291 differentially abundant mRNAs. Clustering of the correlation coefficients of gene expression profiles of all 291 DEGs identified 5 distinct clusters with 4 of them demonstrating significant correlations and forming 4 distinct co-expressed modules (**Fig. 4H** and **Table 3**). (**Fig. 1 and S1**). The diagram in Fig 4H indicates that the 20 differentially abundant mRNAs in cluster 2 (the first that appears on the Fig. 4H diagram) are highly correlated between them and highly anti-correlated with the rest of the inferred clusters and therefore they bare the most informative signal, which might provide possible mechanistic links to the observed cellular phenotypes (Fig. 1 and S1). Remarkably, all mRNAs in cluster 2 (except one) were predicted as hnRNP-C targets (**Fig. 4G**) and are less abundant in the absence of cSetdb1 function (**Table 1**). Further, in line with the observed mESCs survival phenotype, downstream analysis of GO enrichment identified proliferation-related categories, notably Wnt signaling pathway and MAPK activity, including key genes (such as *Dab2* and *Dixdc1*) (**Fig. 4I**).

All these data analyses and prediction show that hnRNP-C, one of the Trim71 partners that we found more associated with Trim71 in absence of Setdb1, targets almost half of the mRNAs that we found differentially abundant upon cSetdb1 function depletion, and provide a potential molecular mechanism through which cSetdb1 regulates gene expression post-transcriptionally.

Overall, the results of the binding , the enrichments and the human/mouse UTR conservation suggest that Setdb1 affects the integrity and the function of Trim71 complex, responsible for the regulation of major pathways, essential for mESC survival and identity.

Discussion

The major H3K9 lysine methyltransferase Setdb1 (mouse Eset) is known to be required for the maintenance and the normal growth of mESCs (Fisher et al., 2017; Lohmann et al., 2010). *Eset* KO embryos lack normal Inner cell mass (ICM), do not form the epiblast, while the extra-embryonic trophectoderm is not affected. Indeed, the inactivation of the mouse gene encoding Setdb1 (*Eset*), induces de-repression of differentiation genes caused by the loss of H3K9 methylation, in particular the trophectoderm genes, inducing the loss of ESC identity. These nuclear roles of Setdb1 in mESCs are thus well studied. However, Setdb1 is localized both in the nucleus and cytoplasm where it is enzymatically active. Our study addressed the potential cytoplasmic role of Setdb1 in mESCs. To this end, we have set a cellular system in which the cytoplasmic fraction of Setdb1 was lost while the nuclear one was maintained. Overall, we found that the cytoplasmic function of Setdb1 is required

for the survival and the normal growth of mESCs. This indicates that cytoplasmic Setdb1 (cSetdb1) regulates ESCs fate independently of its nuclear role..

Next, we asked whether cSetdb1 could regulate gene expression at the post-transcriptional level. Indeed, not only transcription regulation but also post-transcriptional regulations are both fundamental in ESCs fate and identity control (Gabut et al., 2020; Sampath et al., 2008; Schwanhausser et al., 2011). Since Setdb1 has been shown to be associated with ribosomes (Rivera et al., 2015), we first checked whether cSetdb1 could influence protein synthesis. Our data showed that loss of cytoplasmic Setdb1 in mESCs results in a considerable decrease in global ongoing protein synthesis. This was further supported by our proteomic study showing a physical association of Setdb1 with several translational regulators in mESCs. Our data unravel an unsuspected role of Setdb1 in protein synthesis regulation in mESCs. Moreover, the considerable level of protein synthesis dysregulation, observed in a early cSetdb1 LOF timepoint, strongly evokes that as a potential caused of ES cell death.

Next, we asked whether cSetdb1 could regulate mRNA abundance. While the LOF of cSetdb1 function did not induce a significant change in the total mRNA levels, it induced changes in the abundance of specific mRNAs involved in embryogenesis, including development (vascular, reproductive, placenta and somite development), tissue morphogenesis (including also branchial, epithelial and placenta morphogenesis), segmentation and regulation of cellular response to growth factor stimuli. Thus, in addition to the well-described role of Setdb1 in regulating gene expression in the nucleus *via* H3K9 methylation, cSedtb1 seems to be crucial in mRNA abundance regulation in the cytoplasm independently of gene transcription.

Our proteomic study showed that Setdb1 strongly interacts with the RNA-binding protein Trim71, a cytoplasmic key post-transcription regulator in ESCs. Trim71, which is both a E3 ubiquitin ligase and a mRNA silencer, co-localizes with DCP1a in P-bodies (Aeschimann et al., 2017; Rybak et al., 2009), and is required for ESCs self-renewal (Chang et al., 2012; Worringer et al., 2014).

Interestingly, cSetdb1 and Trim71 regulate the abundance of common mRNAs and Trim71 LOF induces similar effect on global protein synthesis as Setdb1 LOF does. These data illustrate the complementary roles and the functional relations that the two partners cSetdb1 and Trim71 have in mESCs.

Setdb1 LOF induced significant changes in Trim71 complex composition, including the presence of many proteins that are involved in mRNA stability and translation: hnRNP-C (RNA-binding protein involved in mRNA turnover and translation, among its different functions, Eif5a2 (translation elongation factor, involved also in mRNA turnover in addition to translation), Gnl3 (associated with proteins responsible of ribosome biogenesis) , Smyd5 (associated with the RNA helicase Mov10, a key protein involved in mRNA silencing together with the RISC complex (Castello et al., 2012)). These

data illustrate that the profile of Trim71 partners, whereby Trim71 executes its cellular functions, is dependent on Setdb1 and provide important mechanistic hypothesis to explain the role of cSetdb1 in post-transcriptional regulation of gene expression, through Trim71.

The top Trim71 partner, whose interaction depends on cSetdb1, is the heterogeneous nuclear ribonucleoprotein hnRNP-C, which is also localized in the cytoplasm where it regulates the translation efficiency of specific mRNAs (Christian et al., 2008; Kim et al., 2003). We observed that more hnRNP-C protein interacts with Trim71 in cSetdb1 LOF condition. Thus, cSetdb1 is essential for a balanced and harmonious interaction between hnRNP-C and Trim71. Moreover, cSetdb1 and hnRNP-C share common mRNA targets. Interestingly, previous studies showed that the human hnRNP-C binds *c-myc* mRNA (Kim et al., 2003; Van Nostrand et al., 2016) in particular on its 5'UTR (Van Nostrand et al., 2016), enhancing c-Myc translation in a global context of partial translation inhibition (Kim et al., 2013). The scanning of all mouse 5' and 3'UTRs for hnRNP-C hits, through RBPmap, has identified that also the mouse Myc mRNA is an hnRNP-C target through the 5'UTR. Interestingly, cSetdb1 loss-of-function induced an increased abundance of cMyc mRNA (RNA-seq). In a global context of translation decrease in cSetdb1 loss-of-function condition, the translation of c-Myc should be sustained, the binding of hnRNP-C in complex with Trim71 provide an attractive molecular mechanism. These data suggest that cSetdb1 regulates c-Myc expression at mRNA level , and potentially at protein level, potentially by acting on Trim71 complex integrity, increasing the recruitment of hnRNP-C on c-Myc mRNA, through Trim71. C-Myc is a known transcription factor, required for ESC self-renewal, maintenance of mESCs identity and iPSC reprogramming. Since c-Myc overexpression can activate apoptotic cell death (McMahon, 2014; Prendergast, 1999), it is tempting to propose that c-Myc overexpression under cSetdb1 loss-of-function could contribute, together with the decrease in the amount of newly synthetized proteins, to the main observed phenotype of ES cell death observed under cSetdb1 loss-of-function.

In conclusion, we showed that cytoplasmic Setdb1 has an essential function, independent of Setdb1 nuclear role, key for ESCs and the regulation of their fate. This essential function is exerted at a post-transcriptional level of gene expression regulation and it can be, at least in part, explained by the interaction with the ESC-specific mRNA silencer Trim71 and the crucial role of Setdb1 for the integrity of Trim71 complex. Our data unravel a new role of Setdb1 in post-transcriptional regulation of gene expression and suggest that the cytoplasmic dysregulations, caused by the loss of cSetdb1 functions, affect ES identity and survival.

Methods

Cell lines and cell culture

Setdb1 conditional knockout (cKO) mESCs are a generous gift form Pr Yoichi Shinkai. Prof (Matsui et al., 2010). Yoichi Shinkai's group genetically modified mES TT2 cells in order to create *Setdb1* cKO and KO alleles. The *Setdb1* cKO allele contains a 3' truncated exon 15 and a stop codon inserted in front of this exon. In order to generate the *Setdb1* cKO allele, exons 15 and 16, which encode the core amino acids of the catalytic domain, have been flanked with two loxP sites recognized by Cre recombinase enzyme. Cre-oestrogen receptor fusion gene Mer-Cre-Mer has been introduced to induce acute *Setdb1* KO after Tamoxifen treatment. Setdb1 cKO mESCs where Setdb1 expression is stably rescued by wild type 3xFlag-Setdb1 (WT) or by the catalytic dead mutant 3xFlag-Setdb1 (CA) were generously given by Prof. Yoichi Shinkai. The catalytic dead mutant was obtained with a single lysine mutation. In the lab, Setdb1 cKO mESCs, where Setdb1 expression is stably rescued by NLS-3xFlag-Setdb1 which localizes only in the nucleus, have been established (3 NLS sequences have been added in order to retain Setdb1 in the nucleus). All mESCs were cultured in Dulbecco's modified Eagle's Medium DMEM (Sigma) supplemented with 15% fetal calf serum (Gibco), 1% penicillin/streptomycin (Sigma), 0.1 mM β-mercaptoethanol (Thermo), 1 mM non-essential amino acids (Sigma), and 1000 U/mL of Leukemia Inhibitory Factor (LIF) (Millipore). All mESC lines were cultured in standard feeder-free conditions with 0.2% gelatin, maintained at 37°C and 8% CO_2. To induce deletion of the Setdb1 cKO allele, mESCs were cultured in 800 nM 4-Hydroxy Tamoxifen (Sigma).

Cloning and generation of stable cell lines

Setdb1 cDNA, in addition to 3 NLS sequences, were cloned into pCAG-3XFLAG-IRESbsd vector used by Pr Yoichi Shinkai lab (the same vector that has been used for to introduce 3xFLAG-WT Setdb1 and 3xFLAG-CA Setdb1). Clones were selected in medium containing Blasticidin (7 mg/mL). Full-length Trim71 cDNA was cloned into pCS2 vector given by Liu Yang, which contains a Myc epitope tag.

Transfection

Plasmids, specifically expressing Myc-Trim71 or GFP-Trim71, were transiently transfected into mESCs using lipofectamine 2000 (Life Technologies). Cells were harvested at 24h post-transfection for immunoprecipitation, immunofluorescence, PLA assay and western blot analysis.

Cell count

Harvested cells were resuspended in media or PBS in 0.2% Trypan Blue. Live cells were counted using countess automated Cell Counter (Invitrogen) according to the manufacturer instructions.

RNA purification and quantitative reverse transcription-PCR (RT-qPCR)

Total RNAs were extracted using RNeasy mini-kit (Qiagen) following manufacturer's procedures. DNase (Qiagen) treatment was performed to remove residual DNA. With High Capacity cDNA Reverse Transcription Kit (Applied Biosystems), 1 µg of total RNAs was reverse-transcribed (RT). Real-time quantitative PCR was performed to analyze relative gene expression levels using SYBR Green Master mix (Promega) following manufacturer indications. Relative expression values were normalized to the housekeeping mRNA *Gapdh*. H20 and RT- were used as negative controls.

RNA-seq

RNA was isolated as described above (RNA purification section). After RNA extraction, the amount of RNAs was quantified by Nanodrop. The quality of the RNA was determined on the Agilent 2100 Bioanalyzer (Agilent Technologies, Palo Alto, CA, USA), the RNA integrity number was above 8 for all the samples. To construct libraries, 1 mg of high-quality total RNA sample was processed using Truseq® stranded total RNA kit (Illumina®). After the removal of ribosomal RNAs (using Ribo-zero® rRNA), confirmed by QC control on pico chipTM on the Agilent 2100 Bioanalyzer (Agilent Technologies, Palo Alto, CA, USA), total RNA molecules are fragmented and reverse-transcribed using random primers. Replacement of dTTP by dUTP during the second strand synthesis will permit to achieve the strand specificity. Addition of a single A base to the cDNA is followed by ligation of adapters. Libraries were quantified by qPCR using the KAPA Library Quantification Kit for Illumina Libraries (KapaBiosystems) and library profiles were assessed using the DNA High SensitivityTMHS kit on an Agilent Bioanalyzer 2100. Libraries were sequenced on an Illumina® Nextseq 500 instrument using 75 base-lengths read V2 chemistry in a paired-end mode.

Bioinformatic analyses of RNA-seq data

All sequenced reads were aligned on the GRCm38.p6 version of mouse genome, obtained from ENSEMBL (Cunningham et al., 2019), using the STAR RNA-seq aligner version 2.5.2b (Dobin et al., 2013). Normalized counts table and Transcripts Per Million (TPMs) were calculated using the Rsubread package version 1.24.1 (Liao et al., 2019). Quality control of samples and sequencing was validated by standard R functions for Principal Component Analysis (PCA) and hierarchical clustering. After fitting the linear model with DESq2, differentially expressed genes (DEGs) were predicted by applying a correction for multiple testing pvalue of 0.01. From the remaining list of genes two groups for downstream analysis were selected: one with log2 Fold Change (log2FC) more than one (log2FC >= 1 and log2FC <= -1) to investigate manually several key genes and a second more strict selection of log2FC more than 1.5 (log2FC >= 1.5 and log2FC <= -1.5) to use for the automated downstream enrichment and clustering analysis. All enrichment analyses including GO, Pathways and WikiGenes enrichment as well as Gene Set Enrichment Analysis (GSEA), and visualizations were performed with

the R package ClusterProfiler (Yu et al., 2012). Clustering of DEG TPMs (Transcripts Per kilobase Millions) was performed by using R base functions for hierarchical and k-means clustering using an array of distance measures and cluster numbers such that robust clusters were obtained. Gene expression correlation matrices for DGEs were calculated by the R package NetCluster and clustering and matrix visualization with the routines of the same package. 3' and 5'UTRs were retrieved for all DEGs by the BioMart service of the ENSEMBL database (Yates et al., 2020) for the mouse C57BL/6NJ strain and all the annotated 3' and 5'UTRs were retrieved. For each gene the longest (or at least >8bps) UTR was selected for the RNA-Binding Protein analysis, which was conducted by using the human/mouse conserved motifs of previously characterized RNA-BPs, as indicated on the online tool RBPmap (Paz et al., 2014). Venn diagram analysis were performed by the R package eulerr.
All analyses were performed in R versions 3.5 (for the DEG identification) and 4.0 for the downstream analysis by using in-house developed scripts available at https://github.com/parisepigenetics/setdb1-downstream-anal.

Annexin V assay

Cells were trypsinized and resuspended in 1X Binding Buffer. 1*10^5 cells were incubated for 15 min at RT under lightless condition in 1X Annexin V binding buffer containing FITC Annexin V and propidium iodide according to FITC Annexin V Apoptosis Detection Kit (BD Biosciences). 10.000 cells were sampled on BD FACSCaliburTM flow cytometer and cells were gated based on forward and side scatter. Fluorescence measurements were detected on the FL1 (Annexin V) and FL2 (PI). Data were analyzed using FlowJo software.

SUnSET assay

mESCs were treated with Puromycin for 20min at 37°C then washed with medium for 20 min at 37°C. After trypsinization and washes in PBS the cells were fixed with 2% formaldehyde (Electron Microscopy Sciences) for 15 min, quench with 50 mM NH4Cl for 10 min and permeabilized with 0.2% Triton X-100 for 5 min. Primary antibody against puromycin and Alexa-488 fluorescent secondary antibody were diluted in NH_4Cl containing 10% SVF serum and incubated with cells for 1 hour each at room temperature. The cells were washed and resuspended in PBS. 10.000 cells were sampled on BD FACSCaliburTM flow cytometer and cells were gated based on forward and side scatter. Fluorescence measurements were detected on the FL1. Data were analyzed using FlowJo software.

Immunofluorescence (IF) and imaging

Cells were grown on glass coverslips coated with laminin 10 mg/ml in PBS for 1 h at 37 °C. mESCs cells were fixed with 4% formaldehyde (Electron Microscopy Sciences) for 20 min, quench with 50

mM NH4Cl for 10 min and permeabilized with 0.5% Triton-X-100 for 5 min. Primary and secondary antibodies were diluted in PBS containing 2% SVF serum and 0.1% Tween and incubated with coverslips overnight at 4°C or 1h at room temperature, respectively. DNA was stained with 1 µg ml−1 DAPI (Life Technology). Coverslips were mounted with Vectashield mounting media (Vector labs). Microscopy was performed using inverted microscope Leica DMI- 6000. Images were taken with the HQ2 Coolsnap motorized by Metamorph software. All images were processed with ImageJ software.

DuoLink

Cells were prepared and fixed as described above (IF section). Primary and secondary antibodies were incubated according manufacturer procedure from Duolink™ In Situ kit (Sigma DUO92101). The addition of Minus and Plus probes, the ligation and the amplification steps were carried out following manufacturer indications. Coverslips were stained with DAPI and mounted, following manufacturer indications. Microscopy was performed using inverted microscope Leica DMI- 6000. Images were taken with the HQ2 Coolsnap motorized by Metamorph software. All images were processed with ImageJ software.

Total protein extract

Cells were lysed in RIPA buffer to which protease and phosphatase inhibitors (Sigma) were added. After 30min of incubation, sonication was performed for 10 min (30 sec ON, 30 sec OFF) at medium frequency (Bioruptor Diagenode). The lysate was centrifugate at 16.10^3 RCF for 10 min. Proteins were quantified using Pierce™ BCA™kit.

Cell fractionation, co-immunoprecipitation and mass spectrometry sample preparation

Cells were lysed in buffer A (20 mM HEPES pH 7, 0.15 mM EDTA, 0.15 mM EGTA, 10 mM KCl), 10% NP40 and SR buffer (50 mM HEPES pH 7, 0.25 mM EDTA, 10 mM KCl, 70% (m/v) sucrose) with the addition of protease and phosphatase inhibitors (Sigma). Cell lysates were centrifuged at 2000 g for 5 min and the supernatant was recovered (cytoplasmic fraction) (as in (Fritsch et al., 2010)). Then high and low salt buffer were added (20 mM Tris-HCl pH 7.65; 0.2 mM EDTA; 25% glycerol; 900 mM NaCl; 1.5 mM MgCl2) to a final NaCl concentration of 300 mM to extract nuclear proteins. The nuclear extracts were next treated with Micrococcal nuclease (0.0125 U/ml) at 37°C during 10 min in addition to 1 mM CaCl2. EDTA was then added to 4 mM final concentration in order to stop the nuclease reaction. Finally, sonication was performed for 10 min (30 sec ON, 30 sec OFF) at medium frequency (Bioruptor Diagenode).

The nuclear and cytoplasmic fractions were ultra-centrifugated at 40000 rpm for 30 min and pre-cleared with protein G-agarose beads (Sigma) during 2h at 4°C. Immunoprecipitations were carried

out overnight at 4°C using 5 µg of each antibody. Ultralink A/G beads (Perbio) were blocked overnight at 4°C with 0,3 % BSA and 0.5 µg/µl ssDNA and then incubated with the immunocomplexes the next day for 2 h at 4°C.

For immunoprecipitation using Myc-Trap technology, the Myc-Trap beads were equilibrated with wash buffer (10 mM Tris pH 7.5, 150 mM NaCl, 0.15 mM EDTA). Immunoprecipitations were carried out for 1 h or overnight at 4°C using 25 µL of Myc-Trap bead slurry.

The immunocomplexes were washed four times in wash buffer and the proteins were eluted in NuPAGE 4X loading buffer (Life Technologies) and 10X reducing agent at 96°C during 5 min. Finally, the samples were examined either by western blot or by mass spectrometry at the Taplin facility (as in (Fritsch et al., 2010)).

Mass spectrometry data analyses

Analysis were performed on triplicates except for KO-Trim71 since one sample was distant from the other samples in PCA and had a very low sum of peptide intensities (Fig. S4A). This sample was removed for the analyses, consequently two samples were used for KO-Trim71. As the Trim 71 interactors are expected to bind only to the GFP-Trim column, only the peptides with 50% of valid values were filtered, and, for the consistency of the results, displaying at least 2 valid values in at least one triplicate, allowing the selection of 826 proteins. Missing values were replaced from normal distribution before scale to interval normalization. ANOVA multi-sample test was done with a FDR of 0.1, and the Post Hoc Tukey's HSD test with a FDR of 0.05.

Western blot

Total, nuclear or cytoplasmic protein extracts, or IP samples were prepared in NuPAGE 4X loading buffer (Life Technologies) and 10X reducing agent and hit at 96°C for 5 min. Separations of proteins were performed using pre-cast polyacrylamide gel cassettes (NuPAGE® Novex® 4-12% Bis-Tris) (Life technologies) and 1X NuPAGE MOPS SDS Running Buffer and transferred into nitrocellulose membranes in 20 mM phosphate transfer buffer (pH 6.7). Membranes were blocked in PBS supplemented with 0.1% Tween 20 and 5% nonfat dried milk and incubated with primary antibodies. Primary antibodies were detected with IRDYE- conjugated secondary antibodies and scanned on the LI-COR imaging system. Quantification of bands was performed with LI-COR software.

Antibodies

Antibodies used in western blot: Setdb1 (Abcam-ab107225), Vinculin (Sigma- V9131), alpha-tubulin (Sigma- T9026), GLP (R&D-PP-B0422-00), Trim71 (Fitzerald-70R-11-707), GFP (Santa Cruz-sc-9996), GM130 (BD-610822), eEF1A (Abcam-ab37969), Rpl5 (GeneTex- GTX101821), beta-actin (Sigma-

A5441), GAPDH (Sigma-G9545), eIF3c (Novusbio-NB100-500), SDHA (CST-11998), Ago2 (Abcam-ab32381), c-Myc (clone 7E18, Sigma).

Antibodies used for immunoprecipitation: Myc-Trap (ChromoteK-yta-20), GFP-Trap (ChromoteK-gta-20), IgG (Santa Cruz).

Antibodies used for SUnSET/FACS analyses: Anti-Puromycin (Millipore-MABE343).

Secondary antibodies for IF: AF488 DONKEYF(AB')2, anti-mouse IgG (H+L) (Invitrogen).

Data availability

All NGS sequencing data that support the findings of this study are available in the BioProject database of NCBI (https://www.ncbi.nlm.nih.gov/bioproject) under the accession number PRJNA547572.

References

Aeschimann, F., Kumari, P., Bartake, H., Gaidatzis, D., Xu, L., Ciosk, R., and Grosshans, H. (2017). LIN41 Post-transcriptionally Silences mRNAs by Two Distinct and Position-Dependent Mechanisms. Molecular cell *65*, 476-489 e474.

An, J., Zhang, X., Qin, J., Wan, Y., Hu, Y., Liu, T., Li, J., Dong, W., Du, E., Pan, C.*, et al.* (2014). The histone methyltransferase ESET is required for the survival of spermatogonial stem/progenitor cells in mice. Cell Death Dis *5*, e1196.

Beyer, S., Pontis, J., Schirwis, E., Battisti, V., Rudolf, A., Le Grand, F., and Ait-Si-Ali, S. (2016). Canonical Wnt signalling regulates nuclear export of Setdb1 during skeletal muscle terminal differentiation. Cell Discov *2*, 16037.

Bilodeau, S., Kagey, M.H., Frampton, G.M., Rahl, P.B., and Young, R.A. (2009). SetDB1 contributes to repression of genes encoding developmental regulators and maintenance of ES cell state. Genes Dev *23*, 2484-2489.

Castello, A., Fischer, B., Eichelbaum, K., Horos, R., Beckmann, B.M., Strein, C., Davey, N.E., Humphreys, D.T., Preiss, T., Steinmetz, L.M.*, et al.* (2012). Insights into RNA biology from an atlas of mammalian mRNA-binding proteins. Cell *149*, 1393-1406.

Chang, H.M., Martinez, N.J., Thornton, J.E., Hagan, J.P., Nguyen, K.D., and Gregory, R.I. (2012). Trim71 cooperates with microRNAs to repress Cdkn1a expression and promote embryonic stem cell proliferation. Nat Commun *3*, 923.

Christian, K.J., Lang, M.A., and Raffalli-Mathieu, F. (2008). Interaction of heterogeneous nuclear ribonucleoprotein C1/C2 with a novel cis-regulatory element within p53 mRNA as a response to cytostatic drug treatment. Mol Pharmacol *73*, 1558-1567.

Cunningham, F., Achuthan, P., Akanni, W., Allen, J., Amode, M.R., Armean, I.M., Bennett, R., Bhai, J., Billis, K., Boddu, S.*, et al.* (2019). Ensembl 2019. Nucleic acids research *47*, D745-D751.

Dobin, A., Davis, C.A., Schlesinger, F., Drenkow, J., Zaleski, C., Jha, S., Batut, P., Chaisson, M., and Gingeras, T.R. (2013). STAR: ultrafast universal RNA-seq aligner. Bioinformatics *29*, 15-21.

Dodge, J.E., Kang, Y.K., Beppu, H., Lei, H., and Li, E. (2004). Histone H3-K9 methyltransferase ESET is essential for early development. Molecular and cellular biology *24*, 2478-2486.

Fisher, C.L., Marks, H., Cho, L.T., Andrews, R., Wormald, S., Carroll, T., Iyer, V., Tate, P., Rosen, B., Stunnenberg, H.G*., et al.* (2017). An efficient method for generation of bi-allelic null mutant mouse embryonic stem cells and its application for investigating epigenetic modifiers. Nucleic acids research *45*, e174.

Fritsch, L., Robin, P., Mathieu, J.R., Souidi, M., Hinaux, H., Rougeulle, C., Harel-Bellan, A., Ameyar-Zazoua, M., and Ait-Si-Ali, S. (2010). A subset of the histone H3 lysine 9 methyltransferases Suv39h1, G9a, GLP, and SETDB1 participate in a multimeric complex. Molecular cell *37*, 46-56.

Gabut, M., Bourdelais, F., and Durand, S. (2020). Ribosome and Translational Control in Stem Cells. Cells *9*.

Kim, J.H., Paek, K.Y., Choi, K., Kim, T.D., Hahm, B., Kim, K.T., and Jang, S.K. (2003). Heterogeneous nuclear ribonucleoprotein C modulates translation of c-myc mRNA in a cell cycle phase-dependent manner. Molecular and cellular biology *23*, 708-720.

Kim, Y., Kim, Y.S., Kim, D.E., Lee, J.S., Song, J.H., Kim, H.G., Cho, D.H., Jeong, S.Y., Jin, D.H., Jang, S.J*., et al.* (2013). BIX-01294 induces autophagy-associated cell death via EHMT2/G9a dysfunction and intracellular reactive oxygen species production. Autophagy *9*, 2126-2139.

Kwon, S.C., Yi, H., Eichelbaum, K., Fohr, S., Fischer, B., You, K.T., Castello, A., Krijgsveld, J., Hentze, M.W., and Kim, V.N. (2013). The RNA-binding protein repertoire of embryonic stem cells. Nature structural & molecular biology *20*, 1122-1130.

Lawson, K.A., Teteak, C.J., Gao, J., Li, N., Hacquebord, J., Ghatan, A., Zielinska-Kwiatkowska, A., Song, G., Chansky, H.A., and Yang, L. (2013). ESET histone methyltransferase regulates osteoblastic differentiation of mesenchymal stem cells during postnatal bone development. FEBS letters *587*, 3961-3967.

Liao, Y., Smyth, G.K., and Shi, W. (2019). The R package Rsubread is easier, faster, cheaper and better for alignment and quantification of RNA sequencing reads. Nucleic acids research *47*, e47.

Loedige, I., Gaidatzis, D., Sack, R., Meister, G., and Filipowicz, W. (2013). The mammalian TRIM-NHL protein TRIM71/LIN-41 is a repressor of mRNA function. Nucleic acids research *41*, 518-532.

Lohmann, F., Loureiro, J., Su, H., Fang, Q., Lei, H., Lewis, T., Yang, Y., Labow, M., Li, E., Chen, T*., et al.* (2010). KMT1E mediated H3K9 methylation is required for the maintenance of embryonic stem cells by repressing trophectoderm differentiation. Stem cells *28*, 201-212.

Loyola, A., Bonaldi, T., Roche, D., Imhof, A., and Almouzni, G. (2006). PTMs on H3 variants before chromatin assembly potentiate their final epigenetic state. Molecular cell *24*, 309-316.

Matsui, T., Leung, D., Miyashita, H., Maksakova, I.A., Miyachi, H., Kimura, H., Tachibana, M., Lorincz, M.C., and Shinkai, Y. (2010). Proviral silencing in embryonic stem cells requires the histone methyltransferase ESET. Nature *464*, 927-931.

McMahon, S.B. (2014). MYC and the control of apoptosis. Cold Spring Harb Perspect Med *4*, a014407.

Paz, I., Kosti, I., Ares, M., Jr., Cline, M., and Mandel-Gutfreund, Y. (2014). RBPmap: a web server for mapping binding sites of RNA-binding proteins. Nucleic acids research *42*, W361-367.

Prendergast, G.C. (1999). Mechanisms of apoptosis by c-Myc. Oncogene *18*, 2967-2987.

Rivera, C., Saavedra, F., Alvarez, F., Diaz-Celis, C., Ugalde, V., Li, J., Forne, I., Gurard-Levin, Z.A., Almouzni, G., Imhof, A*., et al.* (2015). Methylation of histone H3 lysine 9 occurs during translation. Nucleic acids research *43*, 9097-9106.

Rybak, A., Fuchs, H., Hadian, K., Smirnova, L., Wulczyn, E.A., Michel, G., Nitsch, R., Krappmann, D., and Wulczyn, F.G. (2009). The let-7 target gene mouse lin-41 is a stem cell specific E3 ubiquitin ligase for the miRNA pathway protein Ago2. Nat Cell Biol *11*, 1411-1420.

Sampath, P., Pritchard, D.K., Pabon, L., Reinecke, H., Schwartz, S.M., Morris, D.R., and Murry, C.E. (2008). A hierarchical network controls protein translation during murine embryonic stem cell self-renewal and differentiation. Cell Stem Cell *2*, 448-460.

Schmidt, E.K., Clavarino, G., Ceppi, M., and Pierre, P. (2009). SUnSET, a nonradioactive method to monitor protein synthesis. Nat Methods *6*, 275-277.

Schultz, D.C., Ayyanathan, K., Negorev, D., Maul, G.G., and Rauscher, F.J., 3rd (2002). SETDB1: a novel KAP-1-associated histone H3, lysine 9-specific methyltransferase that contributes to HP1-mediated silencing of euchromatic genes by KRAB zinc-finger proteins. Genes Dev *16*, 919-932.

Schwanhausser, B., Busse, D., Li, N., Dittmar, G., Schuchhardt, J., Wolf, J., Chen, W., and Selbach, M. (2011). Global quantification of mammalian gene expression control. Nature *473*, 337-342.

Tan, S.L., Nishi, M., Ohtsuka, T., Matsui, T., Takemoto, K., Kamio-Miura, A., Aburatani, H., Shinkai, Y., and Kageyama, R. (2012). Essential roles of the histone methyltransferase ESET in the epigenetic control of neural progenitor cells during development. Development *139*, 3806-3816.

Torres-Fernandez, L.A., Jux, B., Bille, M., Port, Y., Schneider, K., Geyer, M., Mayer, G., and Kolanus, W. (2019). The mRNA repressor TRIM71 cooperates with Nonsense-Mediated Decay factors to destabilize the mRNA of CDKN1A/p21. Nucleic acids research *47*, 11861-11879.

Van Nostrand, E.L., Pratt, G.A., Shishkin, A.A., Gelboin-Burkhart, C., Fang, M.Y., Sundararaman, B., Blue, S.M., Nguyen, T.B., Surka, C., Elkins, K.*, et al.* (2016). Robust transcriptome-wide discovery of RNA-binding protein binding sites with enhanced CLIP (eCLIP). Nat Methods *13*, 508-514.

Welte, T., Tuck, A.C., Papasaikas, P., Carl, S.H., Flemr, M., Knuckles, P., Rankova, A., Buhler, M., and Grosshans, H. (2019). The RNA hairpin binder TRIM71 modulates alternative splicing by repressing MBNL1. Genes Dev *33*, 1221-1235.

Worringer, K.A., Rand, T.A., Hayashi, Y., Sami, S., Takahashi, K., Tanabe, K., Narita, M., Srivastava, D., and Yamanaka, S. (2014). The let-7/LIN-41 pathway regulates reprogramming to human induced pluripotent stem cells by controlling expression of prodifferentiation genes. Cell Stem Cell *14*, 40-52.

Yang, L., Lawson, K.A., Teteak, C.J., Zou, J., Hacquebord, J., Patterson, D., Ghatan, A.C., Mei, Q., Zielinska-Kwiatkowska, A., Bain, S.D.*, et al.* (2013). ESET histone methyltransferase is essential to hypertrophic differentiation of growth plate chondrocytes and formation of epiphyseal plates. Dev Biol *380*, 99-110.

Yates, A.D., Achuthan, P., Akanni, W., Allen, J., Allen, J., Alvarez-Jarreta, J., Amode, M.R., Armean, I.M., Azov, A.G., Bennett, R.*, et al.* (2020). Ensembl 2020. Nucleic acids research *48*, D682-D688.

Ye, J., and Blelloch, R. (2014). Regulation of pluripotency by RNA binding proteins. Cell Stem Cell *15*, 271-280.

Yeap, L.S., Hayashi, K., and Surani, M.A. (2009). ERG-associated protein with SET domain (ESET)-Oct4 interaction regulates pluripotency and represses the trophectoderm lineage. Epigenetics Chromatin *2*, 12.

You, K.T., Park, J., and Kim, V.N. (2015). Role of the small subunit processome in the maintenance of pluripotent stem cells. Genes Dev *29*, 2004-2009.

Yu, G., Wang, L.G., Han, Y., and He, Q.Y. (2012). clusterProfiler: an R package for comparing biological themes among gene clusters. OMICS *16*, 284-287.

Acknowledgements

We thank Pr Yoishi Shinkai for generous sharing of biological material. We warmly thank Dr Anna Polesskaya and Dr Clément Carré for technical and critical help. Work in Ait-Si-Ali's laboratory was supported by the Fondation pour la Recherche Medicale (FRM, « Equipe FRM » grant # DEQ20160334922); Association Française contre les Myopathies Telethon (AFM-Telethon, grant # 22480); Agence Nationale de la Recherche (ANR, « MuSIC » grant # ANR-17-CE12-0010-01), Université Paris Diderot and the "Who Am I?" Laboratory of Excellence, # ANR-11-LABX-0071, funded by the French Government through its "Investments for the Future" program, operated by the ANR under grant #ANR-11-IDEX-0005-01. R.R. has been supported by a DIM Biotherapies – Paris and nd LABEX "Who am I?" (Université de Paris—Université Paris Diderot) fellwoships. P.C-T. has been supported by the Colombian Administrative Department of Science, Technology and Innovation (COLCIENCIAS-COLFUTURO); Universidad del Rosario (Becas para Apoyo para Estudiantes Doctorales 2017); Colombian Institute of Educational Credit and Technical Studies Abroad (ICETEX); French Government Agency Campus France (Eiffe-l Excellence Scholarship Program); Fondation ARC pour la Recherche sur le Cancer and LABEX "Who am I?" (Université de Paris—Université Paris Diderot).

Author contributions

The study was designed by S.A. and B.C, who also wrote the manuscript with help from all authors. R.R., L.D., S.A., P. C-T., B.C. generated the data. R.R., P. C-T. and L.D. generated the sequencing data which were analyzed by C.B. and B.C.

Additional information

Four Supplementary figures and two supplementary videos accompany this manuscript.

Competing interests

The authors declare no competing interests.

Figure legends

Figure 1. Cytoplasmic Setdb1 is essential for the survival of mESCs.

(**A**) Setdb1 protein level in total protein extracts from ES cells (genetically modified TT2 cells, inducible for an acute *Setdb1* KO through Tamoxifen treatment). Setdb1 expression was analyzed in ES cells (Ctr) and *Setdb1* KO ES cells after 24 hours, 48 hours, 72 hours, and 96 hours of Tamoxifen treatment.

(**B**) *Upper panel*, Setdb1 expression was analyzed after 48-hour-Tamoxifen treatment in *Setdb1* KO ES cells. *Setdb1* inducible KO ES cells stably expressing wild-type Flag-Setdb1 (KO + WT), the enzymatically-dead point mutant (KO + CA), or the nuclear-specific form of Flag-Setdb1 (KO + NLS), and in non-treated ES cells (Ctr). Vinculin or Tubulin is used as western blot loading control. *Lower panel*, Setdb1 protein level obtained from nuclear/cytoplasmic fractionation. GLP is used as a nuclear extraction control; tubulin detection is used as a cytoplasmic extraction control. Setdb1 expression was analyzed in Ctr, KO, KO + WT, KO + CA, KO + NLS.

(**C**) Immunofluorescence using anti-Setdb1 antibody, performed in Ctr, KO and KO + NLS ES cells. Green: Setdb1; red: DAPI.

(**D**) *In vitro* radioactive methylation test using histone H3 within purified nucleosomes as substrate, radioactive S-Adenosyl Methionine (SAM) as methyl donor and immunoprecipitated Setdb1 from the cytoplasmic fractions of Ctr, KO, KO + WT and KO + CA (enzymatically-dead point mutant). Recombinant active full-length Setdb1 was used as positive control (Ctr). *Upper panel*, autoradiography; *lower panel*, western blot.

(**E**) Annexin V FITC Assay to detect apoptotic cells (Annexin V+/PI- and Annexin V+/PI+ cells) in Ctr, KO, KO + WT, KO + NLS ES cells (*Setdb1* KO was obtained after 96 hours of Tamoxifen treatment). FACS data: the quadrant on the lower left includes analyzed living cells (Annexin V-/PI-), the quadrant on the lower right includes cells in the early stage of apoptosis (Annexin V+/PI-), the quadrant on the upper right includes cells in the late stage of apoptosis (Annexin V+/PI+) and in the quadrant on the upper left includes the cells in necrosis (Annexin V-/PI+). FACS data were quantified and represented as scatter plot with bars. N = 4. Statistic test: unpaired t-test *p value < 0.05; **p value < 0.01; ***p value < 0.001; ns=not significant.

(**F**) Live cell number was determined in KO, KO + WT, KO + NLS (*Setdb1* KO was obtained after 96 hours of Tamoxifen treatment), using Trypan Blue staining assay. N=3. Statistic test: t-test *p value < 0.05; **p value < 0.01.

(**G**) Left: Annexin V FITC Assay to detect apoptotic cells (Annexin V+/PI- and Annexin V+/PI+ cells) in KO + WT, KO + NLS, after 6 days of Tamoxifen treatment. FACS data were quantified and represented as scatter plot with bars. N = 3. Statistic test: t-test **p value < 0.01. Right: live cell number was determined in KO + WT, KO + NLS (*Setdb1* KO was obtained after 6 days of Tamoxifen treatment), using Trypan Blue staining assay. N=3. Statistic test: t-test ***p value < 0.001.

Figure 2. Cytoplasmic Setdb1 regulates the abundance of mRNAs and newly synthetized proteins.

(**A**) K-means clustering (k = 2) of the normalized transcripts per million (TMP) of all the 291 differentially expressed genes (DEGS). DEGs were selected for a logFC >= 1.5 and p value< 0.01. On the plot their expression levels in the three KO+WT and the three KO+NLS samples are highlighted, with red highlighting low and green highlighting high expression level. The two groups of DEGs are clearly separated and these two are the only two robust clusters obtained by k-means clustering.

(**B**) Category Network plot (cnetplot) of the top 20 enriched terms from the gene ontology biological processes. Cnetplots represent relationships between biological concepts (here GO Biological Processes) and the genes contained in them. Each different concept link is highlighted with different colors. The size of circles corresponds to the concept enrichment and the green-red gradient for each gene represents its log fold change.

(**C**) DEGs pathway enrichment. DotPlot diagram for pathway enrichment of differentially expressed genes in KO + NLS compared to KO + WT (Fold change > 1.5, p-value < 0.01). Pathways are sorted according to the ratio of the number of DGEs found in each pathway over the number of genes in such pathway (GeneRatio horizontal axis). The color of each circle corresponds to the -corrected for multiple testing- p value of the enrichment test and the size of each circle is equivalent to the number of DEGs found in each pathway.

(**D**) SUnSET experiment performed in Ctr, KO, KO + WT and KO + NLS. *Setdb1* KO condition correspond to 48 hours of Tamoxifen treatment. Cells were treated with 1 μg/mL Puromycin for 20 minutes, then analyzed by FACS after the addition of anti-puromycin antibody and a fluorescent secondary antibody. Several experimental controls were used: cells without any treatment and any antibodies labelling (Ctr-w/o; KO-w/o), cells labeled only with the secondary antibody in order to detect the experiment background (Ctr - II antibody); cells treated with both Puromycin and Cycloheximide, a translation inhibitor (Ctr (Puromycin+CHX)) as negative control. FACS data were quantified (using the median values) and represented as scatter plot with bars. N = 4. Statistic test: t-test *p value < 0.05; **p value < 0.01; ***p value < 0.001; ns: not significant.

Fig 3. Cytoplasmic Setdb1 interacts with Trim71, a mESC-specific regulator of gene expression.

(**A**) Top panel: Directed Yeast-two-hybrid test showing the interaction between Setdb1 and Trim71. Bottom panel: representation of the Trim71 major domains and the domain which mediates the interaction between Trim71 and Setdb1 (in red, aa 358-397).

(**B**) Co-Immunoprecipitation assay performed from the cytoplasmic fraction of ES cells stably expressing flagged WT-Setdb1 and transiently expressing GFP-Trim71 (on the left) or Myc-Trim71 (on the right). Trim71 was detected with anti-GFP (on the left) or anti-Myc and anti-Trim71 (on the right) antibodies and the co- immunoprecipitated Setdb1 was detected with anti-Flag (on the left) or anti-Setdb1 (on the right) antibodies. The plasmid expressing GFP (on the left) or the empty plasmid (on the right, W/O) were used as negative controls. MW: molecular weight marker.

(**C**) *In situ* proximity ligation assay using anti-Myc and anti-GFP antibodies, performed in ES cells transiently expressing Myc-Setdb1 and GFP-Trim71. ES cells transiently expressing Myc-Setdb1 and GFP-Par4 were used as negative control. Green: PLA signal. Red: DAPI. PLA signals were quantified (number of spots) and represented as scatter plot with bars. ****p value < 0.0001.

(**D**) *In situ* proximity ligation assay using anti-Setdb1 and anti-Dcp1a performed in ES cells. Anti-GM130 was used as negative control Green: PLA signal. Red: DAPI. PLA signals were quantified (number of spots) and represented as scatter plot with bars. ****p value < 0.0001.

(E) Venn diagram showing the numbers and overlap of RNAs that are differentially abundant between KO+WT and KO+NLS (differentially expressed genes (DEGs) were selected for a logFC >= 1.5 and p-value< 0.01) and differentially regulated genes after *Trim71*-KO (PMID: 31371437).

(**F**) RT-qPCR for endogenous *Ccnd2*, *H60b*, *Ccnd1*, *Inhbb* mRNAs performed in Ctr, KO, KO + WT, KO + NLS to validate RNAseq. N=3. Statistic test: t-test *p value < 0.05; **p value < 0.01; ***p value < 0.001; ****p value < 0.0001; ns=not significant.

(**G**) SUnSET experiment performed in Ctr and Trim71 KD cells. Trim71 KD was obtained after 72 hours of siRNA treatment. N=4. Statistic test: t-test **p value < 0.01.

Figure 4. Integrity of Trim71 complex(es), involved in mRNA stability and translation, is affected in the absence of Setdb1.

(**A-B**) GFP-Trim71 (Trim71) was immunoprecipitated from the cytoplasmic fractions of control or *Setdb1* KO ES cells. GFP (Ctr) was used as a control of the immunoprecipitation. (**A**) Silver staining to

detect proteins of immunoprecipitated proteins. (**B**) The amount of immunoprecipitated proteins Trim71 and GFP in ES or KO cells, was checked by Western Blot.

(**C**) PCA analysis. ES-Ctr (cross), KO-Ctr (diagonal cross), ES-Trim71 (square), KO-Trim71 (filled square).

(**D**) Differential analysis (multiple sample test ANOVA) after quantification of almost 800 proteins of which 108 are differentially enriched at FDR < 0.1 level. Heatmap after clustering of these significant proteins with the sum of their intensities.

(**E**) Heatmap after clustering of the significant proteins with the score obtained by the Tukey's honestly significant difference (THSD, B).

(F) List of gene names of the mRNAs that are differentially expressed in KO+WT and found associated to hnRNP-c by eCLIP, see text for details. Number refers to LogFC.

(G) Venn diagram showing the clusters of the 157 mRNAs differentially abundant in absence of cSetdb1 function and the mRNAs whose 3'UTR are potential binding site of hnRNP-C.

(H) Clustered correlation plot reveals 4 distinct co-expressed modules. Soft-thresholded correlation matrix of the 291 DEG TPMs clustered by hierarchical clustering and the Ward D2 linkage identifies the structure of 5 modules (the 5th module containing the rest 117 DEGs with relatively low correlation, was excluded from the figure). Each module represents a set of co-expressed genes which might also be co-regulated.

(I) GO enrichment DotPlot of the second co-expressed module (Cluster 2) of the correlation plot of panel H. Enrichment identifies GO categories related to MAPK activation and WNT signaling. Again (like in Fig. 2) categories are sorted according to GeneRatios and color and size correspond to the corrected p value and the gene count for each category.

- Table 1: List of RNAs differentially abundant in KO+NLS compared to KO+WT cells (log2FC more than 1.5, see Material and methods). Numbers refers to TPM values for each sample. In the logFC1 tab, genes names in bold refers to genes that are also Trim71 targets and belong to the ontology "multicellular organismal reproductive process" in a ToppGene analysis (toppgene.cchmc.org).

- Table 2: Table of the 128 out of the 291 differentially between KO+WT and KO+NLS (Fig. 2, differentially expressed genes were selected for a logFC >= 1.5 and p value< 0.01), and that are targets RNAs of hnRNP-C (Van Nostrand et al., 2016). Numbers refers to Log2 fold change KO+WT/KO+NLS in RNAseq and eCLIP/input for CLIP experiment.

- Table 3: Gene composition of the clusters described in Figure 4G-I.

Figures

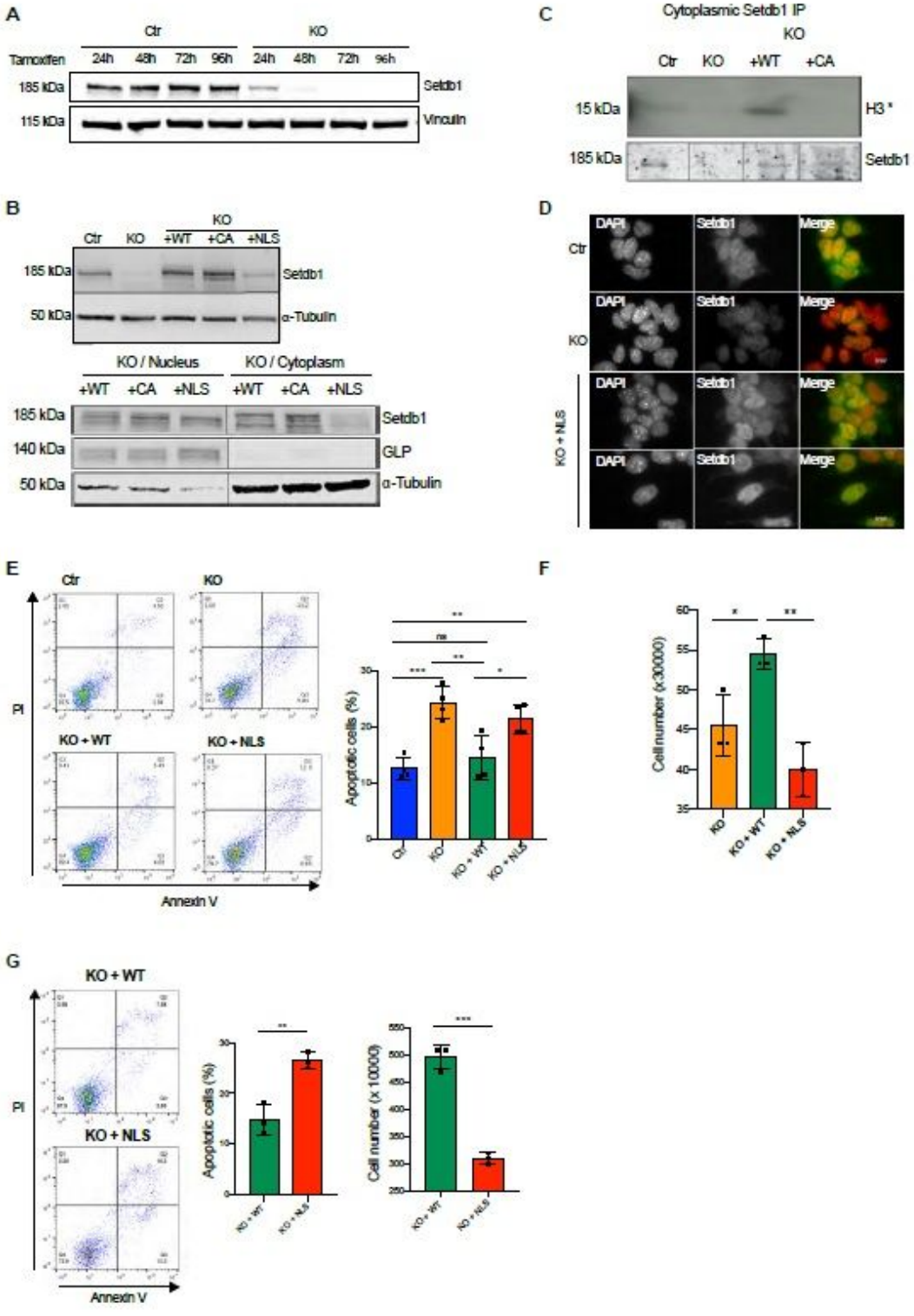

Figure 1

Cytoplasmic Setdb1 is essential for the survival of mESCs. (A) Setdb1 protein level in total protein extracts from ES cells (genetically modified TT2 cells, inducible for an acute Setdb1 KO through Tamoxifen treatment). Setdb1 expression was analyzed in ES cells (Ctr) and Setdb1 KO ES cells after 24

hours, 48 hours, 72 hours, and 96 hours of Tamoxifen treatment. (B) Upper panel, Setdb1 expression was analyzed after 48-hour-Tamoxifen treatment in Setdb1 KO ES cells. Setdb1 inducible KO ES cells stably expressing wild-type Flag-Setdb1 (KO + WT), the enzymatically-dead point mutant (KO + CA), or the nuclear-specific form of Flag-Setdb1 (KO + NLS), and in non-treated ES cells (Ctr). Vinculin or Tubulin is used as western blot loading control. Lower panel, Setdb1 protein level obtained from nuclear/cytoplasmic fractionation. GLP is used as a nuclear extraction control; tubulin detection is used as a cytoplasmic extraction control. Setdb1 expression was analyzed in Ctr, KO, KO + WT, KO + CA, KO + NLS. (C) Immunofluorescence using anti-Setdb1 antibody, performed in Ctr, KO and KO + NLS ES cells. Green: Setdb1; red: DAPI. (D) In vitro radioactive methylation test using histone H3 within purified nucleosomes as substrate, radioactive S-Adenosyl Methionine (SAM) as methyl donor and immunoprecipitated Setdb1 from the cytoplasmic fractions of Ctr, KO, KO + WT and KO + CA (enzymatically-dead point mutant). Recombinant active full-length Setdb1 was used as positive control (Ctr). Upper panel, autoradiography; lower panel, western blot. (E) Annexin V FITC Assay to detect apoptotic cells (Annexin V+/PI- and Annexin V+/PI+ cells) in Ctr, KO, KO + WT, KO + NLS ES cells (Setdb1 KO was obtained after 96 hours of Tamoxifen treatment). FACS data: the quadrant on the lower left includes analyzed living cells (Annexin V-/PI-), the quadrant on the lower right includes cells in the early stage of apoptosis (Annexin V+/PI-), the quadrant on the upper right includes cells in the late stage of apoptosis (Annexin V+/PI+) and in the quadrant on the upper left includes the cells in necrosis (Annexin V-/PI+). FACS data were quantified and represented as scatter plot with bars. N = 4. Statistic test: unpaired t-test *p value < 0.05; **p value < 0.01; ***p value < 0.001; ns=not significant. (F) Live cell number was determined in KO, KO + WT, KO + NLS (Setdb1 KO was obtained after 96 hours of Tamoxifen treatment), using Trypan Blue staining assay. N=3. Statistic test: t-test *p value <0.05; **p value < 0.01. 23 (G) Left: Annexin V FITC Assay to detect apoptotic cells (Annexin V+/PI- and Annexin V+/PI+ cells) in KO + WT, KO + NLS, after 6 days of Tamoxifen treatment. FACS data were quantified and represented as scatter plot with bars. N = 3. Statistic test: t-test **p value < 0.01. Right: live cell number was determined in KO + WT, KO + NLS (Setdb1 KO was obtained after 6 days of Tamoxifen treatment), using Trypan Blue staining assay. N=3. Statistic test: t-test ***p value < 0.001.

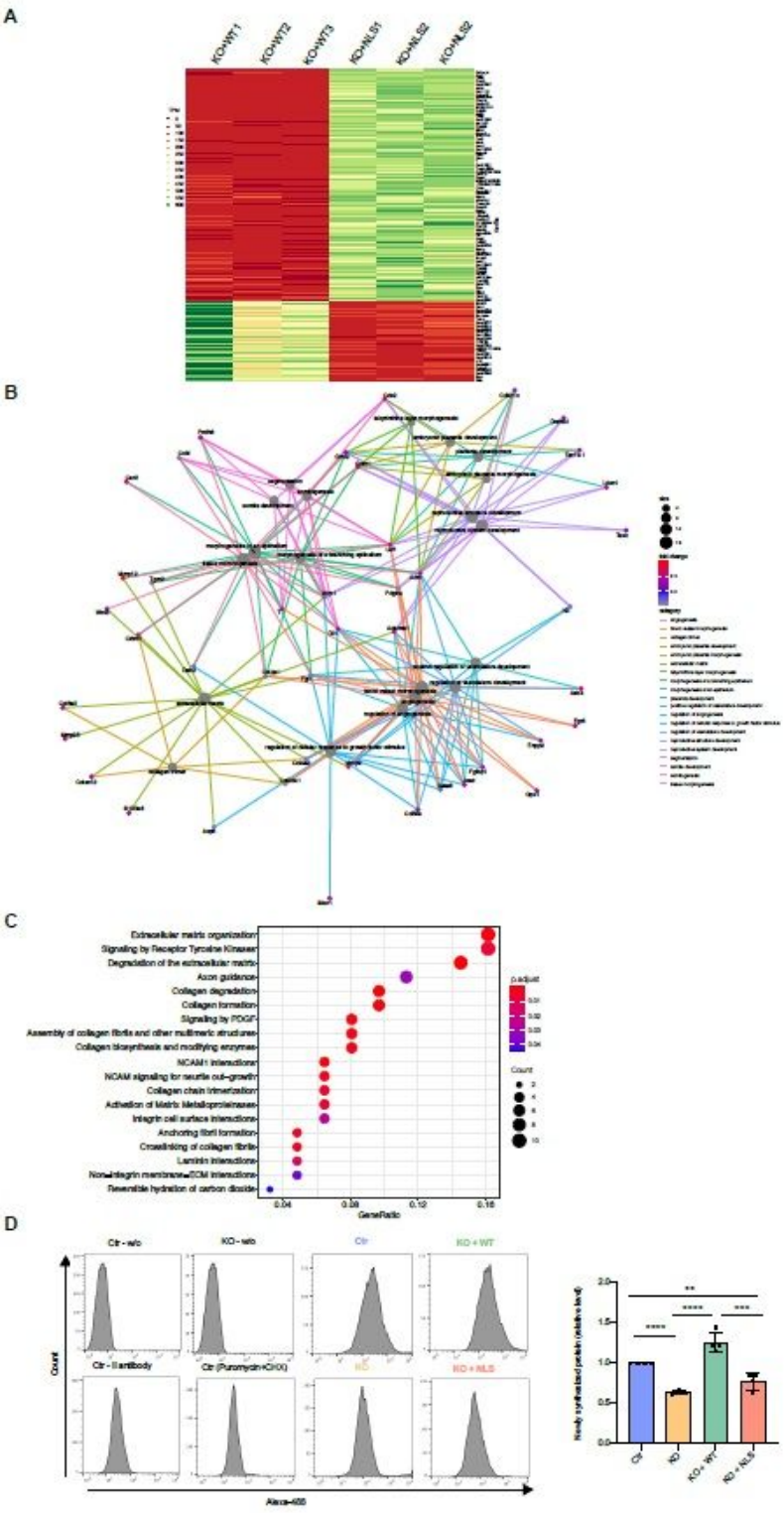

Figure 2

Cytoplasmic Setdb1 regulates the abundance of mRNAs and newly synthetized proteins. (A) K-means clustering (k = 2) of the normalized transcripts per million (TMP) of all the 291 differentially expressed genes (DEGS). DEGs were selected for a logFC >= 1.5 and p value< 0.01. On the plot their expression levels in the three KO+WT and the three KO+NLS samples are highlighted, with red highlighting low and green highlighting high expression level. The two groups of DEGs are clearly separated and these two are

the only two robust clusters obtained by k-means clustering. (B) Category Network plot (cnetplot) of the top 20 enriched terms from the gene ontology biological processes. Cnetplots represent relationships between biological concepts (here GO Biological Processes) and the genes contained in them. Each different concept link is highlighted with different colors. The size of circles corresponds to the concept enrichment and the green-red gradient for each gene represents its log fold change. (C) DEGs pathway enrichment. DotPlot diagram for pathway enrichment of differentially expressed genes in KO + NLS compared to KO + WT (Fold change > 1.5, p-value < 0.01). Pathways are sorted according to the ratio of the number of DGEs found in each pathway over the number of genes in such pathway (GeneRatio horizontal axis). The color of each circle corresponds to the -corrected for multiple testing- p value of the enrichment test and the size of each circle is equivalent to the number of DEGs found in each pathway. (D) SUnSET experiment performed in Ctr, KO, KO + WT and KO + NLS. Setdb1 KO condition correspond to 48 hours of Tamoxifen treatment. Cells were treated with 1 µg/mL Puromycin for 20 minutes, then analyzed by FACS after the addition of anti-puromycin antibody and a fluorescent secondary antibody. Several experimental controls were used: cells without any treatment and any antibodies labelling (Ctr-w/o; KO-w/o), cells labeled only with the secondary antibody in order to detect the experiment background (Ctr - II antibody); cells treated with both Puromycin and Cycloheximide, a translation inhibitor (Ctr (Puromycin+CHX)) as negative control. FACS data were quantified (using the median values) and represented as scatter plot with bars. N = 4. Statistic test: ttest *p value < 0.05; **p value < 0.01; ***p value < 0.001; ns: not significant.

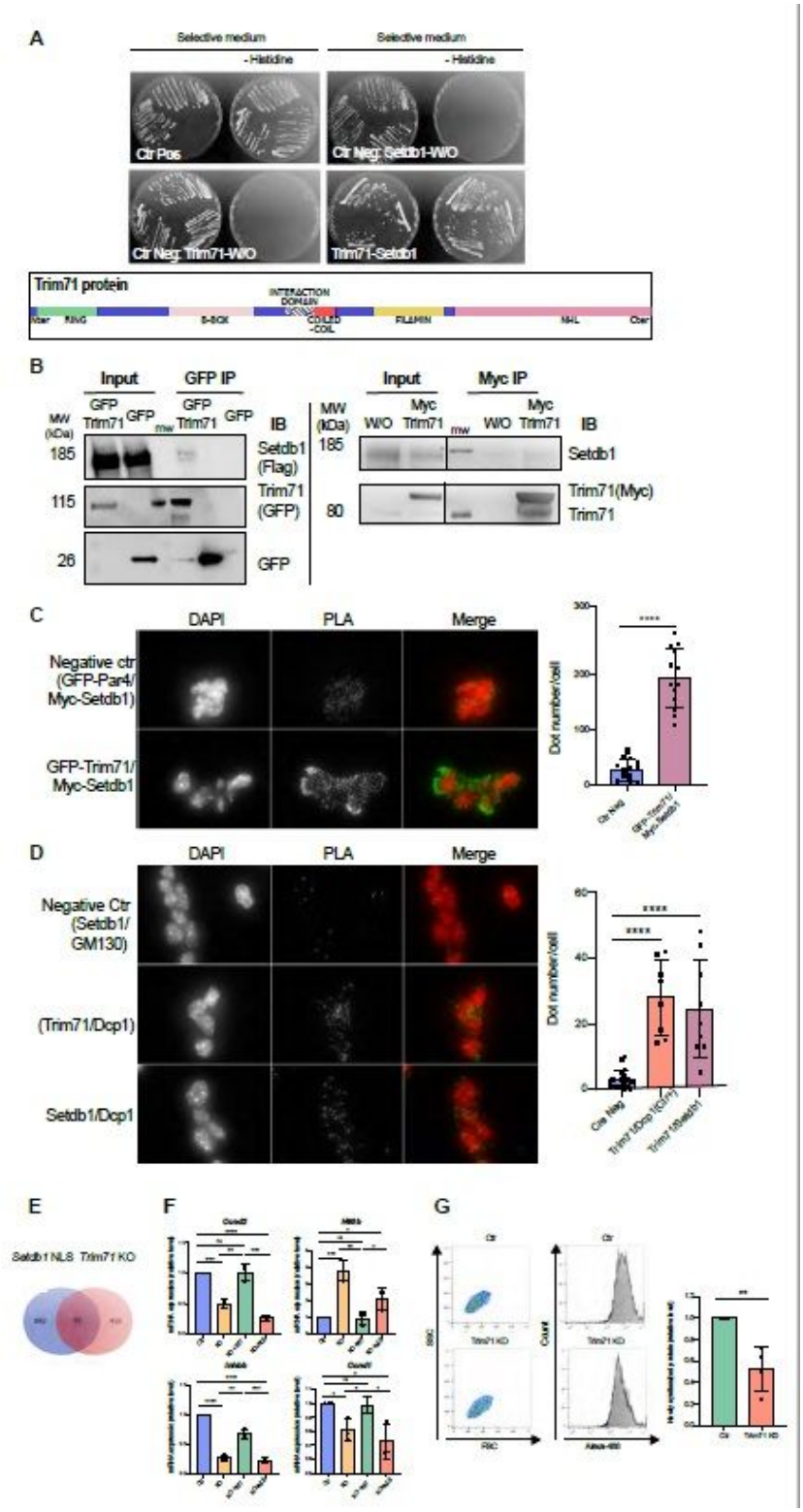

Figure 3

Cytoplasmic Setdb1 interacts with Trim71, a mESC-specific regulator of gene expression. (A) Top panel: Directed Yeast-two-hybrid test showing the interaction between Setdb1 and Trim71. Bottom panel: representation of the Trim71 major domains and the domain which mediates the interaction between Trim71 and Setdb1 (in red, aa 358-397). (B) Co-Immunoprecipitation assay performed from the cytoplasmic fraction of ES cells stably expressing flagged WT-Setdb1 and transiently expressing GFP-

Trim71 (on the left) or Myc-Trim71 (on the right). Trim71 was detected with anti-GFP (on the left) or anti-Myc and anti-Trim71 (on the right) antibodies and the co- immunoprecipitated Setdb1 was detected with anti-Flag (on the left) or anti-Setdb1 (on the right) antibodies. The plasmid expressing GFP (on the left) or the empty plasmid (on the right, W/O) were used as negative controls. MW: molecular weight marker. (C) In situ proximity ligation assay using anti-Myc and anti-GFP antibodies, performed in ES cells transiently expressing Myc-Setdb1 and GFP-Trim71. ES cells transiently expressing Myc-Setdb1 and GFP-Par4 were used as negative control. Green: PLA signal. Red: DAPI. PLA signals were quantified (number of spots) and represented as scatter plot with bars. ****p value < 0.0001. (D) In situ proximity ligation assay using anti-Setdb1 and anti-Dcp1a performed in ES cells. Anti-GM130 was used as negative control Green: PLA signal. Red: DAPI. PLA signals were quantified (number of spots) and represented as scatter plot with bars. ****p value < 0.0001. (E) Venn diagram showing the numbers and overlap of RNAs that are differentially abundant between KO+WT and KO+NLS (differentially expressed genes (DEGs) were selected for a logFC >= 1.5 and p-value< 0.01) and differentially regulated genes after Trim71-KO (PMID: 31371437). (F) RT-qPCR for endogenous Ccnd2, H60b, Ccnd1, Inhbb mRNAs performed in Ctr, KO, KO + WT, KO + NLS to validate RNAseq. N=3. Statistic test: t-test *p value < 0.05; **p value < 0.01; ***p value < 0.001; ****p value < 0.0001; ns=not significant. (G) SUnSET experiment performed in Ctr and Trim71 KD cells. Trim71 KD was obtained after 72 hours of siRNA treatment. N=4. Statistic test: t-test **p value < 0.01.

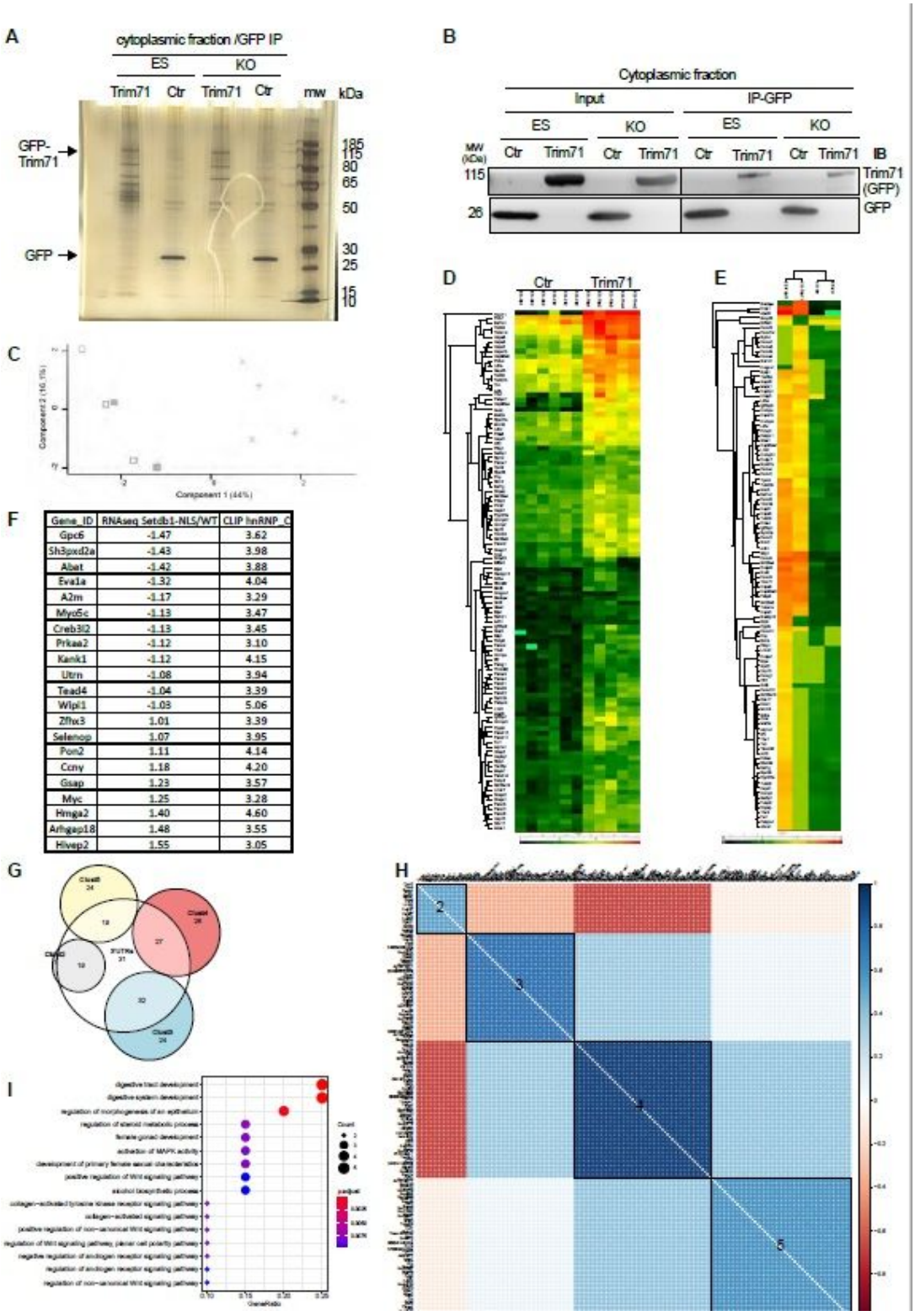

Figure 4

Integrity of Trim71 complex(es), involved in mRNA stability and translation, is affected in the absence of Setdb1. (A-B) GFP-Trim71 (Trim71) was immunoprecipitated from the cytoplasmic fractions of control or Setdb1 KO ES cells. GFP (Ctr) was used as a control of the immunoprecipitation. (A) Silver staining to detect proteins of immunoprecipitated proteins. (B) The amount of immunoprecipitated proteins Trim71 and GFP in ES or KO cells, was checked by Western Blot. (C) PCA analysis. ES-Ctr (cross),

KO-Ctr (diagonal cross), ES-Trim71 (square), KO-Trim71 (filled square). (D) Differential analysis (multiple sample test ANOVA) after quantification of almost 800 proteins of which 108 are differentially enriched at FDR < 0.1 level. Heatmap after clustering of these significant proteins with the sum of their intensities. (E) Heatmap after clustering of the significant proteins with the score obtained by the Tukey's honestly significant difference (THSD, B). (F) List of gene names of the mRNAs that are differentially expressed in KO+WT and found associated to hnRNP-c by eCLIP, see text for details. Number refers to LogFC. (G) Venn diagram showing the clusters of the 157 mRNAs differentially abundant in absence of cSetdb1 function and the mRNAs whose 3'UTR are potential binding site of hnRNP-C. (H) Clustered correlation plot reveals 4 distinct co-expressed modules. Soft-thresholded correlation matrix of the 291 DEG TPMs clustered by hierarchical clustering and the Ward D2 linkage identifies the structure of 5 modules (the 5th module containing the rest 117 DEGs with relatively low correlation, was excluded from the figure). Each module represents a set of co-expressed genes which might also be co-regulated. (I) GO enrichment DotPlot of the second co-expressed module (Cluster 2) of the correlation plot of panel H. Enrichment identifies GO categories related to MAPK activation and WNT signaling. Again (like in Fig. 2) categories are sorted according to GeneRatios and color and size correspond to the corrected p value and the gene count for each category.

Supplementary Files

This is a list of supplementary files associated with this preprint. Click to download.

- Table1Raponeetal.xlsx
- Table2Raponeetal.xlsx
- Table3Raponseetal.xlsx
- VideoS1Raponeetal.avi
- VideoS2Raponeetal.avi
- SuppfiguresRaponeetal.pdf